



STUDY THE PERFORMANCE OF CIRCULAR CLARIFIER IN EXISTING POTABLE WATER TREATMENT PLANT BY USING COMPUTATIONAL FLUID DYNAMICS.

Hasim A. M. Heikal

Prof. Dr. in Mech. Power Depart., Faculty of Engineering (Mattaria), Helwan University

Aida A. El-Hafiz

Prof. Dr. in Mech. Power Depart., Faculty of Engineering (Mattaria), Helwan University

Ahmed R. El Baz

Prof. Dr. Mech. Power Depart., Faculty of Engineering, Ain Shames University

Sherif M. Farghaly

Ph.D. in Mech. Power Eng., Faculty of Engineering (Mattaria), Helwan University

ABSTRACT

To account for factors influence the performance of the clarifier, mathematical models may be utilised. In this respect, Computational Fluid Dynamics (CFD) model enables the investigation of internal processes, such as local velocities and solids concentrations, to identify process inefficiencies. Then, using 2D CFD and SST k- ω model with DPM method, a numerical simulation of flow in the tank was developed by Fluent Software to study and investigate the flow field and performance of the sedimentation tank at the Armant water treatment in Qena Governorate, Egypt.

Key Words: Clarifier, Clarifications, sedimentation tank, Computational fluid dynamics, settling tank, Numerical modelling.

1. INTRODUCTION

Solids removal is probably the main water purification method in water treatment plants. The most significant phase of this process is to separate sludge and suspended particles from water by means of gravity. In these basins, the turbid water flows into the basin at one end and the cleaner water is taken out at the other end by decanting. Obviously, the water must flow in the tank long enough for the appropriate particle deposition. Sedimentation by gravity is a usual and important process in settling tanks to remove inorganic settleable solids from water and waste water in refinery plants (Swamee and Tyagi 1990).

Numerous studies show that in order to remove suspended solids with minimum cost; they should be removed as quickly and efficiently as possible from the water. In fact, if the removed solid concentrations from settling tanks are increased in order to increase treatment efficiency, the size of water treatment facilities, which are located downstream of the clarifiers, can be reduced (Cripps et al, 2000). According to the investigations of Camp (1946) and Swamee and Tyagi (1990), the investment costs of settling facilities contribute to a large portion (typically one-fourth to one-third) of the total cost of treatment plant construction. For that reason, significant savings in both capital and operational costs at various stages of treatment can be expected by increasing solid removal efficiency (Cripps et al, 2000). As a result, increasing removal efficiency is important.



Many factors can influence removal efficiency, including tank hydraulics, which are of great significance (De Clercq et al, 2003). It is noticeable that the ability of a sedimentation tank to remove suspended solids depends on its flow field. Therefore, investigating the structure of the flow field is of great importance [Campbell and Empie, 2006].

Goula et al 2008 said that to improve the design of process equipment while avoiding tedious and time consuming experiments computational fluid dynamics (CFD) calculations have been employed during the last decades. Fluid flow patterns inside process equipment may be predicted by solving the partial differential equations that describe the conservation of mass and momentum. The geometry of sedimentation tanks makes analytical solutions of these equations impossible, so usually numerical solutions are implemented using computational fluid dynamics packages. The advent of fast computers has improved the accessibility of CFD, which appears as an effective tool with great potential. Regarding sedimentation tanks, CFD may be used first for optimizing the design and retrofitting to improve effluent quality and underflow solids concentration. Second, it may increase the basic understanding of internal processes and their interactions. This knowledge can again be used for process optimization. The latter concerns the cost-effectiveness of a validated CFD model where simulation results can be seen as numerical experiments and partly replace expensive field experiment (Huggins, et al 2005).

Matko et al (1996) reviewed the recent progress in numerical modelling techniques applied to sedimentation tanks in wastewater treatment and mentioned that the important CFD modelling criteria for the settling of suspended solids in sedimentation tanks are the velocity distribution, settling velocity distribution of suspended solids, turbulent mass diffusion of suspended solids, re-suspension of settled solids from tank base, temperature effects, flow variation, effect of flow on floc growth or breakup, wind effects on the water surface, and movement of scrapers. Burt et al (2005) studied the internal hydrodynamic behaviour of final clarifiers by using the Computational Fluid Dynamics (CFD). A central EDI helps to diffuse the density current by spreading the load uniformly near the top of the stilling well and reducing the density gradients in the stilling pond. Benedek et al (2007) studied the one-dimensional (1-D) model of the secondary settling tank (SST), and the drive for model development was discussed using steady-state simulation results generated with a 2-D computational fluid dynamics (CFD) model. Fan et al (2007) studied the flow dynamics in a secondary sedimentation tank. The solid-liquid two-phase turbulent flow in the tank modelled with the three-dimensional two-fluid model. Michael et al (2007) presented a computational fluid dynamics (CFD) model that predicts the sedimentation of activated sludge in a full-scale flat-bottom circular secondary clarifier that was equipped with a suction-lift sludge removal system.

Goula et al (2008) studied the effect of adding a vertical baffle at the feed section of a full-scale sedimentation tank for the improvement of solids settling in potable water treatment by using CFD model. Abbas et al (2010) studied the improvement of the operation and performance of Water Treatment Plant by improving circular sedimentation tanks of Al-Gazaer Water Treatment Plants in Al Dewanyia city in Iraq which have been identified as operating poorly. Ghawi et al (2011) also examined the modification of inlet baffles through the use of an energy dissipating inlet (EDI) to

enhance the performance in the circular Secondary clarifiers at the Al-Dewanyia wastewater treatment plant in Iraq.

For modelling the particle transport, De Clercq and Vanrolleghem (2002) mentioned that the Lagrangian model should not be applied whenever the particle volume fraction exceeds 10–12%.

In general, many researchers have used CFD simulations to describe water flow and solids removal in settling tanks for sewage water treatment. However, works in CFD modelling of sedimentation tanks for potable water treatment are very limited in the literature. Moreover, the physical characteristics of the flocs may not be such significant parameters in the flow field of clarifiers for potable water, due to the much lower solids concentrations and greater particle size distributions than those encountered in wastewater treatment.

The objective of this work was to study and analysis the performance of the sediment transport for multiple particle sizes in full-scale sedimentation tanks of potable water treatment plants.

2. GOVERNING EQUATION

2.1 Time averaged flow equations

The governing equations that determine flow are the general mass continuity and momentum expressions. The turbulence model is also used to calculate the Reynolds stresses. The mass continuity equation for fluid is simple: as the flow pattern is assumed to be two dimensional (2D), two momentum equations in the x and r directions respectively represent the length and height of the tank to be solved. The flows occurring in a rectangular sedimentation tank, the governing equations for two-dimensional mean flow are as follows:

Continuity equation:

$$\frac{\partial \rho}{\partial t} + \frac{\partial}{\partial x_i}(\rho u_i) = 0 \quad (1)$$

Momentum Equations:

$$\frac{\partial}{\partial t}(\rho u_i) + \frac{\partial}{\partial x_j}(\rho u_i u_j) = -\frac{\partial p}{\partial x_i} + \frac{\partial}{\partial x_j} \left[\mu \left(\frac{\partial u_i}{\partial x_j} + \frac{\partial u_j}{\partial x_i} - \frac{2}{3} \delta_{ij} \frac{\partial u_l}{\partial x_l} \right) \right] + \frac{\partial}{\partial x_j}(-\overline{\rho u_i' u_j'}) \quad (2)$$

They have the same general form as the instantaneous Navier-Stokes equations, with the velocities and other solution variables now representing ensemble-averaged (or time averaged) values. Additional terms now appear that represent the effects of turbulence.

These Reynolds stresses, $-\overline{\rho u_i' u_j'}$ must be modelled in order to close Equation (2).

The Reynolds-averaged approach to turbulence modelling requires that the Reynolds stresses in Equation (2) are appropriately modelled. A common method

employs the Boussinesq hypothesis to relate the Reynolds stresses to the mean velocity gradients:

$$-\overline{\rho u'_i u'_j} = \mu_t \left(\frac{\partial u_i}{\partial x_j} + \frac{\partial u_j}{\partial x_i} \right) - \frac{2}{3} \left(\rho k + \mu_t \frac{\partial u_k}{\partial x_k} \right) \delta_{ij} \quad \dots\dots\dots(3)$$

Where k is the turbulent kinetic energy, and μ_t is the turbulent or eddy viscosity. Whereas the dynamic viscosity μ is a fluid property, the eddy viscosity strongly depends on the state of turbulence.

2.2 The SST k- ω Turbulence model

The transport equations for the SST k- ω Turbulence model as follows (Fluent's 14.5 User Guide):

Kinematic Eddy Viscosity

$$\nu_T = \frac{a_1 k}{\max(a_1 \omega, SF_2)} \quad \dots\dots\dots(4)$$

Turbulence Kinetic Energy

$$\frac{\partial k}{\partial t} + U_j \frac{\partial k}{\partial x_j} = P_k - \beta^* k \omega + \frac{\partial}{\partial x_j} \left[(\nu + \sigma_k \nu_T) \frac{\partial k}{\partial x_j} \right] \quad \dots\dots\dots(5)$$

Specific Dissipation Rate

$$\frac{\partial \omega}{\partial t} + U_j \frac{\partial \omega}{\partial x_j} = \alpha S^2 - \beta \omega^2 + \frac{\partial}{\partial x_j} \left[(\nu + \sigma_\omega \nu_T) \frac{\partial \omega}{\partial x_j} \right] + 2(1 - F_1) \sigma_{\omega 2} \frac{1}{\omega} \frac{\partial k}{\partial x_i} \frac{\partial \omega}{\partial x_i} \quad \dots\dots\dots(6)$$

Closure Coefficients and Auxiliary Relations

$$F_2 = \tanh \left[\left[\max \left(\frac{2\sqrt{k}}{\beta^* \omega y}, \frac{500\nu}{y^2 \omega} \right) \right]^2 \right]$$

$$P_k = \min \left(\tau_{ij} \frac{\partial U_i}{\partial x_j}, 10\beta^* k \omega \right)$$

$$F_1 = \tanh \left\{ \left\{ \min \left[\max \left(\frac{\sqrt{k}}{\beta^* \omega y}, \frac{500\nu}{y^2 \omega} \right), \frac{4\sigma_{\omega 2} k}{CD_{k\omega} y^2} \right] \right\}^4 \right\}$$

$$CD_{k\omega} = \max \left(2\rho\sigma_{\omega 2} \frac{1}{\omega} \frac{\partial k}{\partial x_i} \frac{\partial \omega}{\partial x_i}, 10^{-10} \right)$$

$$\phi = \phi_1 F_1 + \phi_2 (1 - F_1)$$

$$\alpha_1 = \frac{5}{9}, \alpha_2 = 0.44$$

$$\beta_1 = \frac{3}{40}, \beta_2 = 0.0828$$

$$\beta^* = \frac{9}{100}$$

$$\sigma_{k1} = 0.85, \sigma_{k2} = 1$$

$$\sigma_{\omega1} = 0.5, \sigma_{\omega2} = 0.856$$

3. CHARACTERISTICS OF THE EXISTING CLARIFIERS

A full-scale circular sedimentation tank will be studied in this work, similar to those used in the potable water treatment plant (WTP) of the city of Armant, Qena , Egypt. The plant receives raw water from Nile River and its capacity is around 34,000 m³/day. The employed processes include intake structure and pumping station, coagulation– flocculation, sedimentation, filtration through sand, sludge treatment, and chlorination. The location of the Armant WTP is shown as the Google image in Figure 1.0.



Figure 1.0 Satellite image for Armant WTP (34,000m³/day), Qena, Egypt.

The two Clari-flocculators (flocculation and sedimentation tanks) in the existing plant are centre-fed type with peripheral weirs. The bottom floors have a steep slope of 2° and a blade scraper pushes the sludge towards a central conical sludge hopper. The dimensions of the tank are shown in Figure 2.0. Clariflocculators are combination of both flocculation as well as clarification. With this, the installation of plant becomes economical and faster. All these Clariflocculators are best suited for water treatment plant, waste treatment plant and effluent treatment plant. The tank consists of a flocculation zone, inside the cone, a clarification zone, outside the cone, a sedimentation zone at the tank bottom, bottom scrapers to convey the settled sludge to the central drain well (Sludge hoper), radial ditches to collect the clarified water.

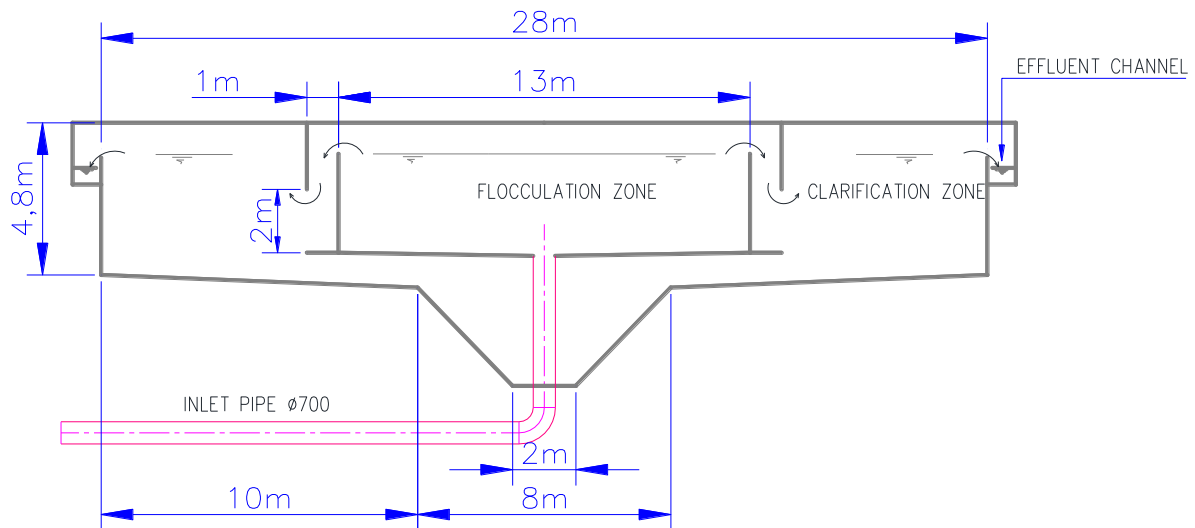


Figure 2.0 The Dimensions of the Clariflocculators at Armant WTP, Qena, Egypt.

In the Clariflocculator, the suspension is flocculated inside the flocculation cylinder by means of slow mixers no. 4 (at 90° from each other). The reagents are added directly into the water to be treated, before it enters the Clariflocculator. The flocculation, which takes place inside the cylinder, makes the suspended particles gather and grow. The flocs in suspension, which come out of the flocculation cylinder, tend to sediment. The clarified water is collected in the upper part through a circular ditch. The flocs settled on the bottom are conveyed to the central drain well by scrapers.

4. NUMERICAL MODEL

Steady-state incompressible flow conditions with viscous effects are generally considered in hydraulic numerical modelling, and the Navier–Stokes equation has been well modified to solve the governing equation. The Navier–Stokes equation is an incompressible form of the conservation of mass and momentum equations, and is comprised of non-linear advection, rate of change, diffusion, and source terms in the partial differential equation. The mass and momentum equations joined through velocity can be used to obtain an equation for the pressure term. When the flow field is turbulent, the computation becomes more complex. Hence, the RANS equations, which are modified forms of the Navier–Stokes equation including the Reynolds stress term, which approximates the random turbulent fluctuations by statistics, are prevalently used.

In this study, the available computational fluid dynamics (CFD) program Fluent 14.5, developed by Ansys, was used for the numerical simulation. Fluent solves the RANS equations by the finite volume formulation obtained from a rectangular finite difference grid. For each cell, the average values of the flow parameters, such as pressure and velocity, are computed at discrete times. The new velocity in each cell is calculated from the coupled momentum and continuity equations using previous time step values in each center of the face of cells. The pressure term is obtained and adjusted using the estimated velocity to satisfy the continuity equation. With the computed velocity and pressure for later time, the remaining variables, including turbulent transport, density advection and diffusion, and wall function evaluation, are estimated.

4.1 Model Assumptions:

1. The flow field is the same for all angular positions; therefore, a 2D geometry can be used to properly simulate the general features of the hydrodynamic processes in the tank.
2. The water free surface was modelled as a fixed surface; this plane of symmetry was characterized by zero normal gradients for all variables.
3. The particle mass loading in a sedimentation tank for potable water treatment and primary sedimentation tanks is typically small, and therefore, it can be safely assumed that the presence of particles does not affect the flow field (one-way coupling).
4. The particle diameter is assumed to be constant and to be the average of the lower and upper diameters of the class.
5. The coagulation due to differential settling can be ignored due to the relatively low settling velocities resulting by the low densities of the flocs.

5.1 The Operating Conditions

The inlet was specified as a plug flow of water at velocity of 0.036m/s whereas the inlet turbulence intensity was set at 4.5%. The outlet was specified as a constant pressure outlet with a turbulence intensity of 6.0%.

The water flow rate was 0.222 m³/s based on this rate, the inlet flow rate of particles was estimated as 0.055 kg/s using a measured solids concentration of 250 mg/l, whereas the primary particle density was 1066 kg/m³.

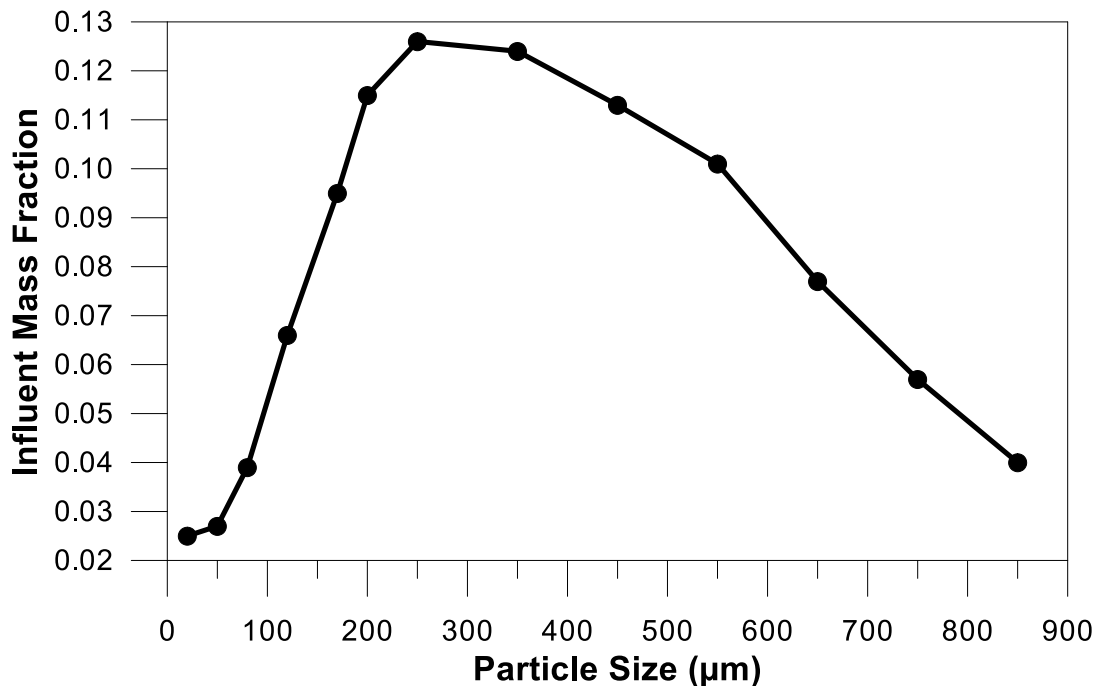


Figure 3.0 Particle size distributions in the influent of the standard sedimentation tank, Goula et al (2008a).

The settling tank was simulated for a specific particle size distribution at the inlet as presented by Goula et al (2008a) in order to evaluate the performance of the settling tank. The range of the suspended solids was divided into 13 distinct classes of particles based on the discretization of the measured size distribution Figure 3.0. Within each class the particle diameter is assumed to be constant.

5.2 Sedimentation Tank Geometry

The tank dimensions according to Figure (2.0) will be summarized in Table 1.0.

Table (1.0) The Dimensions of the existing the Clariflocculator at Armant WTP.

Item	Value	Unit
Inner diameter	13	m
Outer diameter	28	m
Side wall water depth	3.70	m
Inlet opening	0.15	m
Outlet opening	0.12	m

The geometry and main dimension of the sedimentation tank under consideration is shown in Figure 4.0.

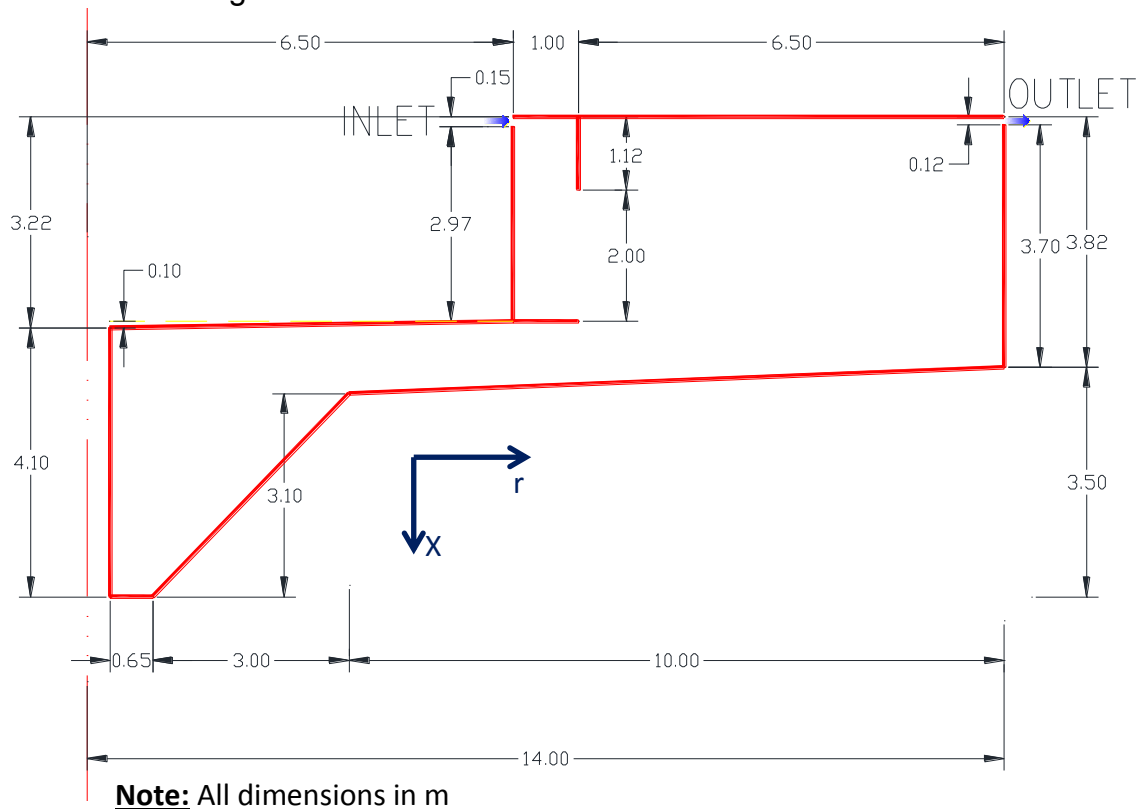


Figure 4.0 Schematic representation of simulated Clari-flocculator.

5.3 Mesh Generation

A grid dependency study was performed to eliminate errors due to the coarseness of the grid and also to determine the best compromise between simulation accuracy, numerical stability, convergence, and computational time. The selected grid was comprised of 152,953 quadrilateral elements.

5.4 Boundary Conditions

The above governing equations form a set of partial differential equations. In order to obtain a unique solution, this set needs to be linked to a set of boundary conditions. The boundary conditions include:

1. The inlet was specified as a uniform velocity, k and ω values (i.e velocity Inlet). Whereas the inlet turbulence intensity was set at 4.5%.
2. The overflow outlets were specified in the top row of cells on either side of the overflow weirs. The outlet is specified as a constant pressure outlet with a turbulence intensity of 6.0%.
3. The vertical and horizontal walls were specified as wall boundaries.
4. The water level is a static free surface was specified as a rigid lid symmetry axis. The variables that were not specified according to a rigid lid symmetry axis were the concentration (for which a zero flux boundary was applied) and the kinetic energy dissipation.

4.1 Simulation Setup

The setup of the CFD modelling by using Fluent 14.5 will be as follows:

a) Solver

Type	: Pressure-Based
Velocity Formation	: Absolute
Time	: Steady
2D Space	: Planer
Gravity acceleration	: 9.81 m/sec in x-direction.

b) Model

Viscous Model	: k- ω (2eqn), SST
---------------	---------------------------

c) Boundary Conditions

Boundary	Item	Values
Inlet	Type	Velocity Inlet
	Velocity Magnitude (m/sec)	0.036
	Turbulent Intensity (%)	4.5
	Hydraulic Diameter (m)	2.793
	Discrete Phase BC type	Escape
Outlet	Type	Pressure Outlet
	Gauge Pressure (pascal)	0
	Turbulent Intensity (%)	6
	Hydraulic Diameter (m)	3.66
	Discrete Phase BC type	Escape
Side Walls	Type	Wall
	Wall Motion	Stationary Wall
	Shear Condition	No Slip
	Discrete Phase BC type	Reflect
Tank Top	Type	Symmetry
Horizontal Baffle at inlet zone & Tank Bottom	Type	Wall
	Wall Motion	Stationary Wall
	Shear Condition	No Slip
	Discrete Phase BC type	Trap

e) Solution

Solution Method

Pressure-Velocity Coupling	:	PISO
Skewness Correction	:	1
Neighbour Correction	:	1

Spatial - Discretization

Pressure	:	Standard
Momentum	:	Second Order Upwind
Turbulent Kinetic Energy	:	Second Order Upwind
Specific Dissipation Rate	:	Second Order Upwind

Solution Controls

Under-Relaxation Factor

Pressure	:	0.6
Density	:	1
Body Force	:	1
Momentum	:	0.8
Turbulent Kinetic Energy	:	0.9
Specific Dissipation Rate	:	0.8
Turbulent Viscosity	:	1

Monitors

Residual	:	10^{-6}
----------	---	-----------

5. RESULTS AND DISCUSSION

The main objective of this section is to present the results of the basic study and to investigate hydraulic characteristics and performance of the sedimentation tank as well as the removal/settling efficiency.

5.1 Flow Pattern

The removal efficiency in settling tanks depends on the physical characteristics of the suspended solids as well as on the flow field and the mixing regime in the tank. Therefore the determination of flow and mixing characteristics is essential for the prediction of the tank efficiency. Figure 5.0 presents the predicted streamlines for the tank. The displayed simulations were made without solids present.

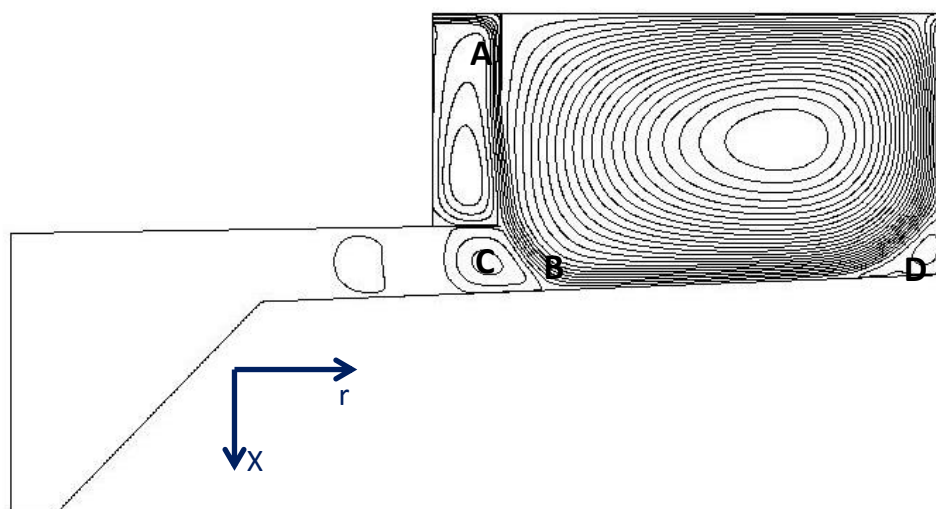


Figure 5.0 Predicated streamlines for the sedimentation tank.

The influent, after impinging on the flow control baffle at point A, is deflected downwards to the tank bottom. The flow splits at point B on the bottom of the tank, producing a recirculation eddy at C. Generally, the flow pattern is characterized by a large recirculation region spanning a large part of the tank from top to bottom. Three smaller recirculation regions are also found as follows;

- Small recirculation at the top of the tank near the entry points of the liquid stream.
- Small recirculation at the bottom left-hand side of the tank just under the horizontal baffle at inlet zone where the sludge gathers before moving toward the sludge hopper.
- Small recirculation the bottom right-hand side of the tank just under the exit region.

These regions have a substantial impact on the hydrodynamics and the efficiency of the sedimentation tank.

The same behaviour was observed by Goula et al 2008 and Stamou (1991) in their flow velocity predictions in a settling tank.

All the above behaviour and currents are agreed with the current results of the velocity profiles inside the sedimentation tank, see Figure 8.0.

5.2 Turbulent Kinetic Energy (k)

The kinetic energy contours present works are shown in Figure 6.0

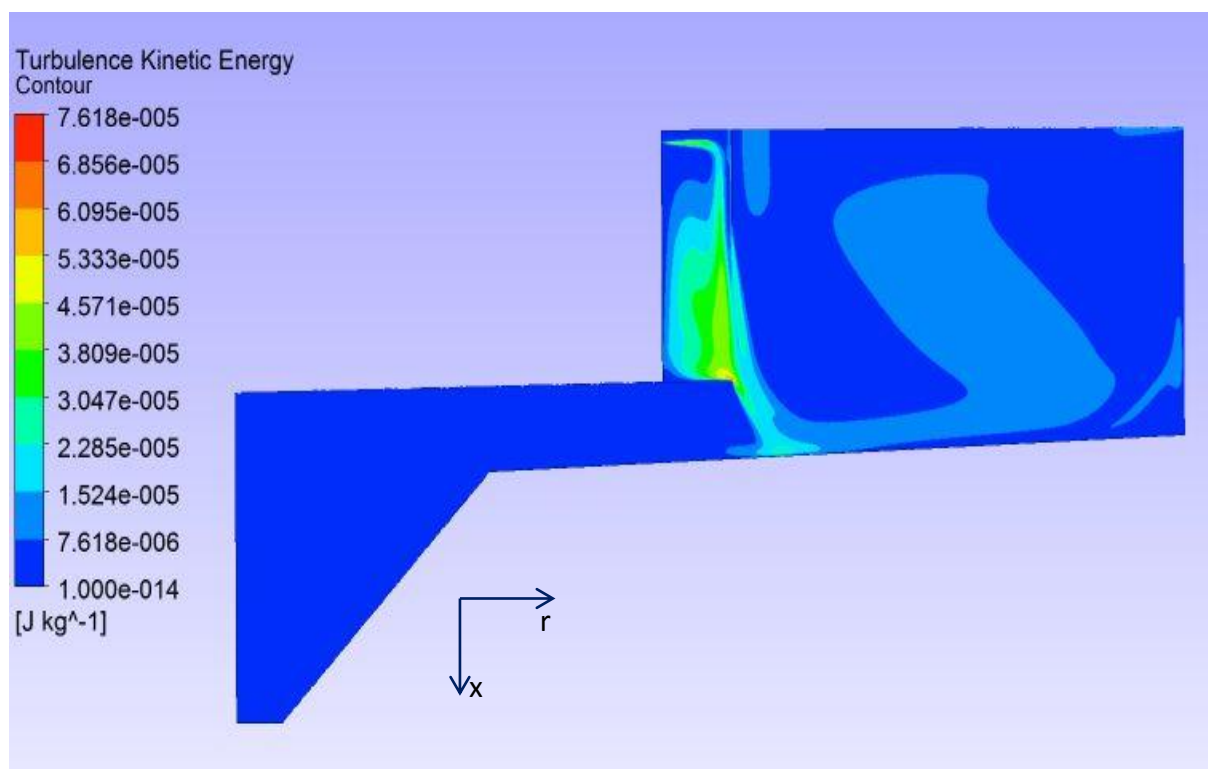


Figure 6.0 Contours of turbulent kinetic energy ($\text{m}^2 \text{s}^{-2}$) for the sedimentation tank.

As observed by Goula et al 2008a, the kinetic energy of the incoming flow is dissipated due to the presence of inlet baffle.

5.3 Velocity Contours

The velocity contours inside the sedimentation tank are shown in Figure 7.0.

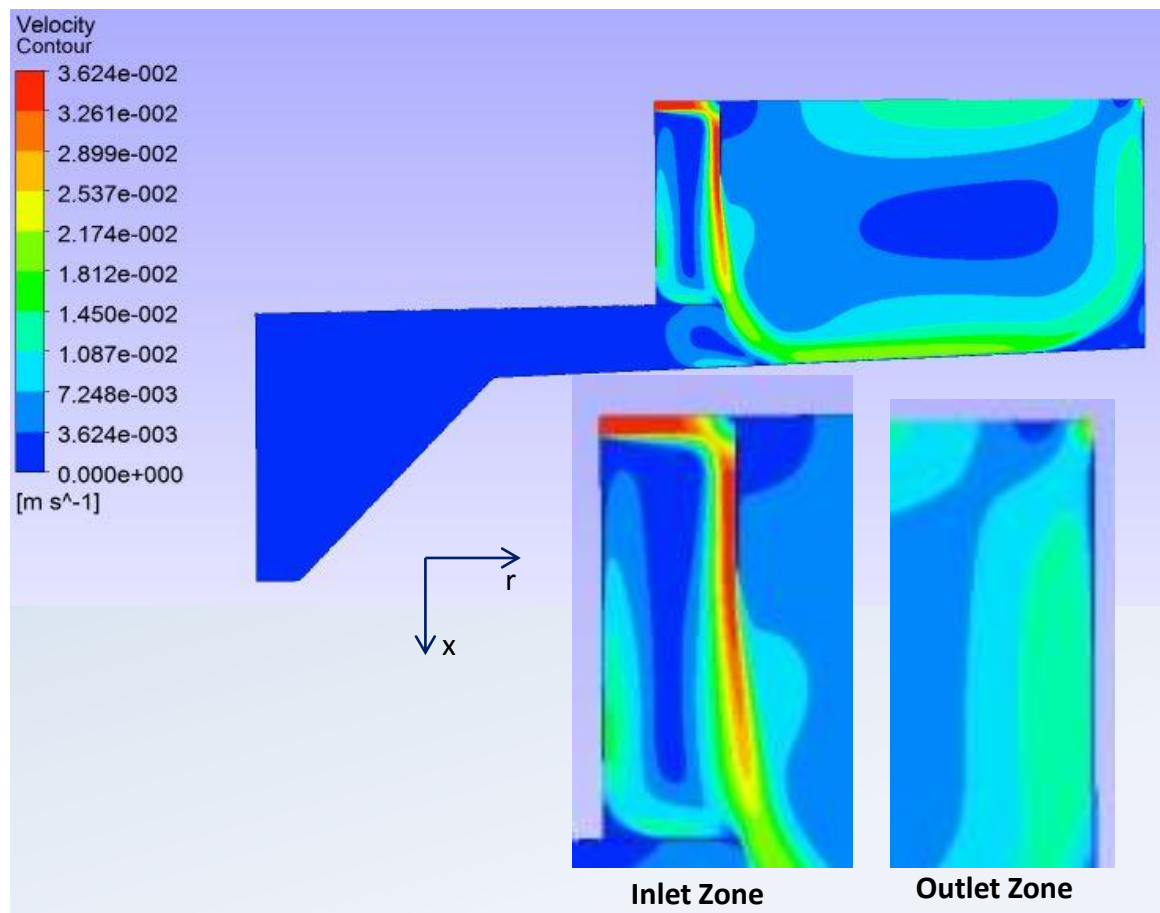


Figure 7.0 Contours of velocity inside the sedimentation tank

The flow pattern predicted by the model in the inlet zone shows some of the characteristics of free jet flow near the front of the inlet port, i.e., it is still strongly dependent on the momentum of the influent. As shown in Figure 7.0, the influent jet impinges on the reaction baffle (skirt) and then is deflected downward to the bottom of the tank, thus a strong downward current appears near the section of the skirt. At this section the position of the maximum radial velocity is near the bottom of the sedimentation tanks. The horizontal velocities under the reaction baffle section are non-uniform. The flow pattern in the settling zone is quite sensitive to this velocity profile; Figure 5.0 indicates that two eddies occur in association with the bottom current. One of the eddy is located inside the inlet zone while the other eddy occurs downstream of the reaction baffle (at under the horizontal baffle at inlet). The space occupied by the inlet zone eddy is greater for the neutral density flow and decreases with increasing density difference. The other important features of the inlet zone are high mixing, high dissipation of kinetic energy, and entrainment of flow from the settling zone.

5.4 Velocity Profiles

The radial velocity (U_r) inside the Sedimentation tank at different radial locations (r) against the position is presented in Figure 8.0.

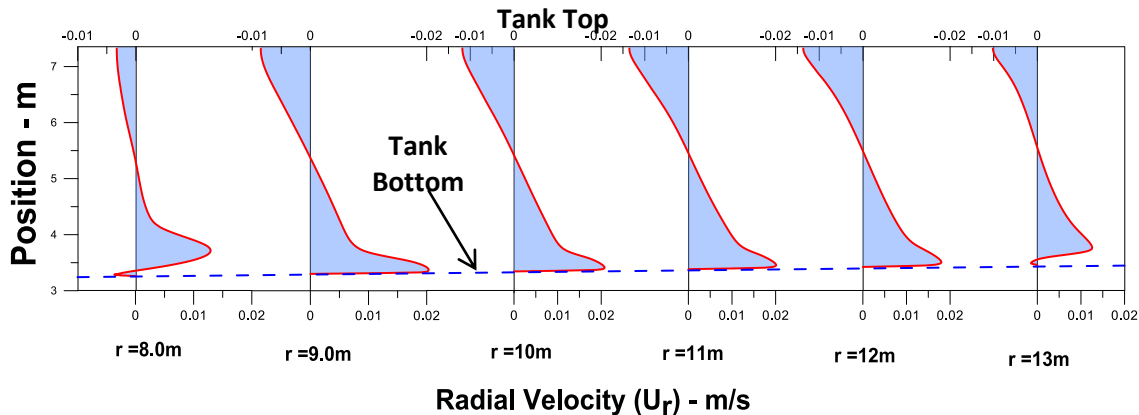


Figure 8.0 Velocity profile inside the sedimentation tank at different radial location.

As shown in Figure 8.0, the forward flow velocities is located in the zone close to the tank bottom and backward flow velocities is located in the upper zone of the tank close to the top. The forward velocity at the inlet zone (at $r=9$) is higher than that in the outlet region.

5.5 Flocs (Solids) Distributions

Figure 9.0 shows the flocs concentration profile along the tank bottom for different particle Class size. The results are in a good agreement with the results obtained by Goula et al (2008a).

In Figure 10, the zero position of the horizontal axis is set at the left-hand end of the tank bottom. Clearly, the increase the particular size allows the solids to settle at much short distances from the left-hand corner of the tank (at inlet region after baffle). On the whole, the simulation results demonstrate quantitatively the drastic effect of particle velocity on sedimentation effectiveness. Higher settling velocities lead to more effective sedimentation. However, even small differences in particle settling velocity can cause large changes in the percent of settled particles.

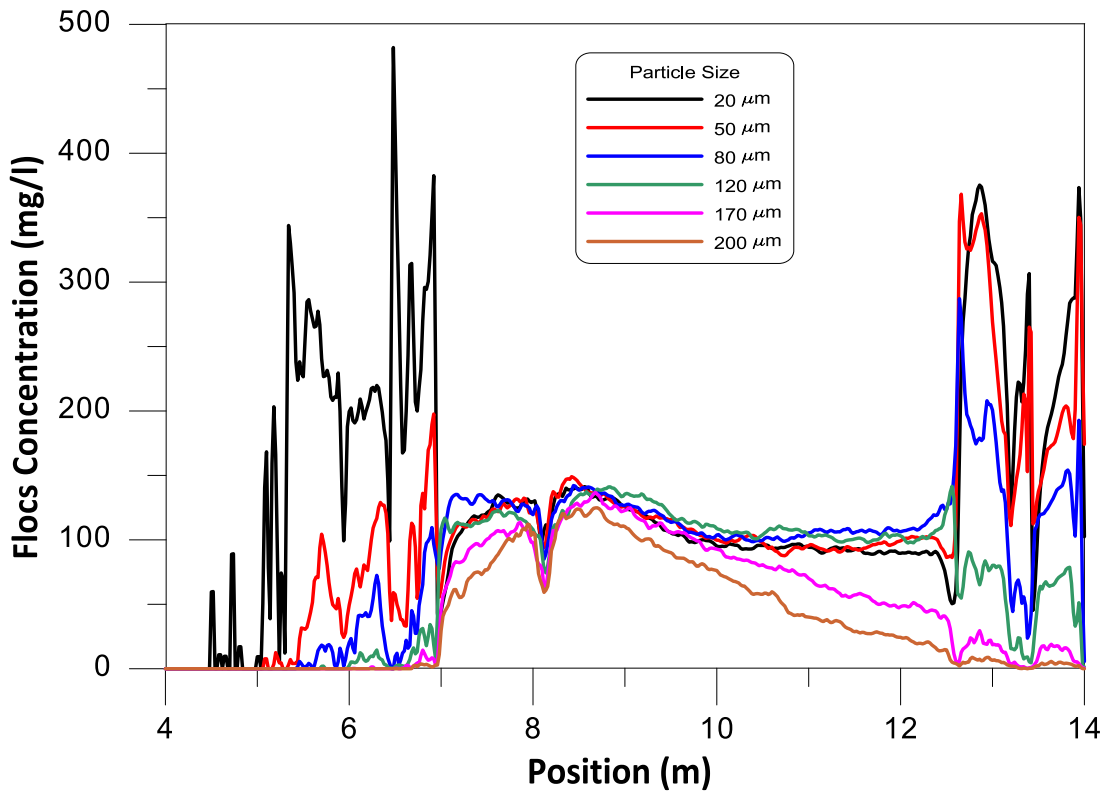


Figure 9.0 Flocs concentration (mg/l) along the tank bottom for different particle class sizes.

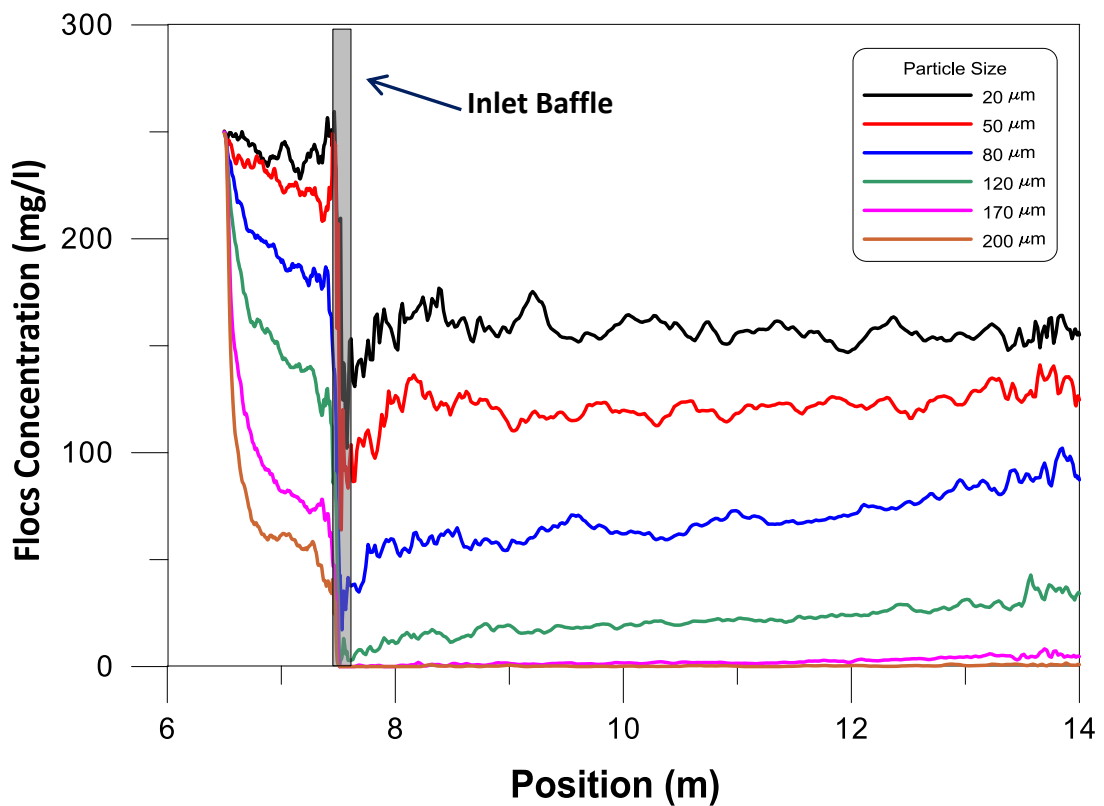


Figure 10 Flocs concentration (mg/l) along the tank top for different particle class sizes.

Figure 10 shows the flocs concentration profile along the tank top for different particle class size. At the inlet region, the flocs concentrations at tank top will be equal regardless the particular size.

The concentration will decrease as the distance from the inlet increases. The increase in the particular size allows the solids to settle at much short distances from the left-hand corner of the tank (at inlet region after baffle). Therefore, the flocs concentration at tank top will be reduced when the particle size increase.

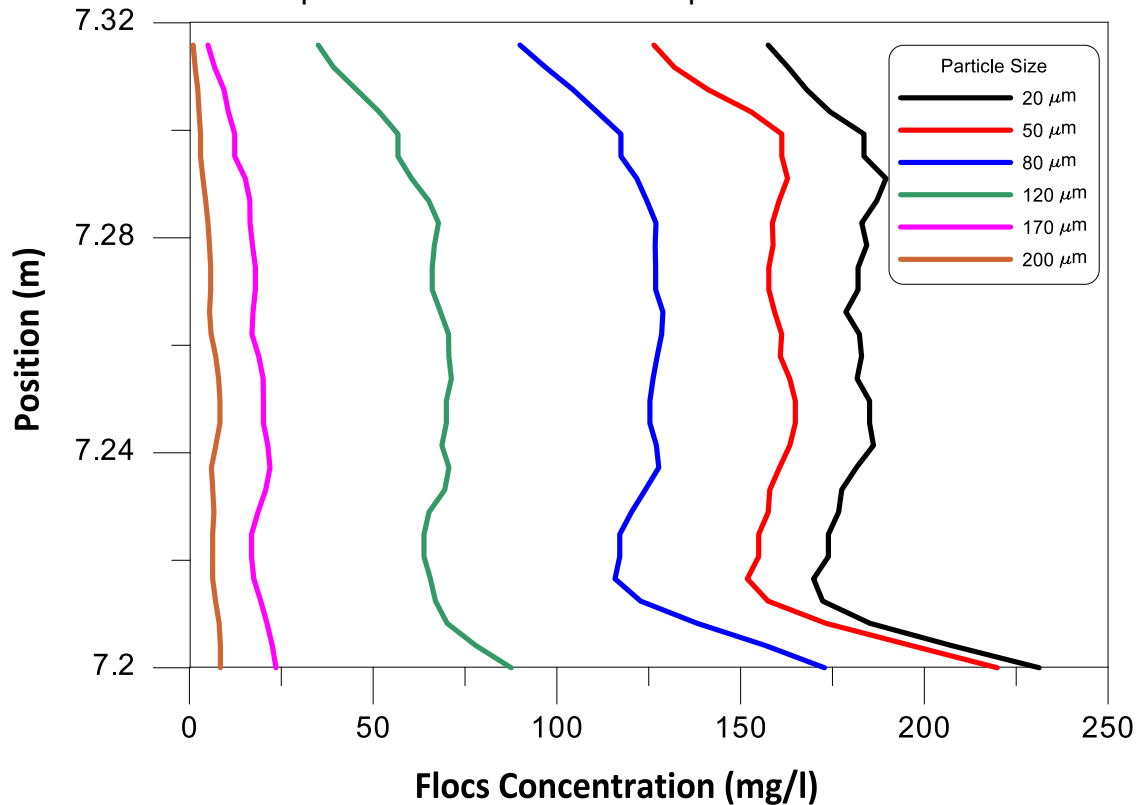
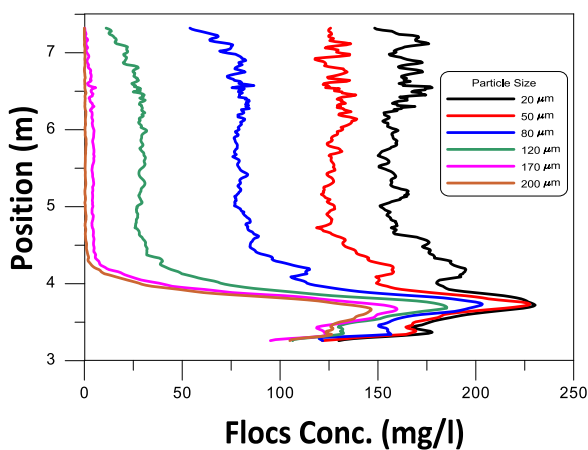


Figure 11 Flocs concentration profile at tank outlet for different particle sizes.

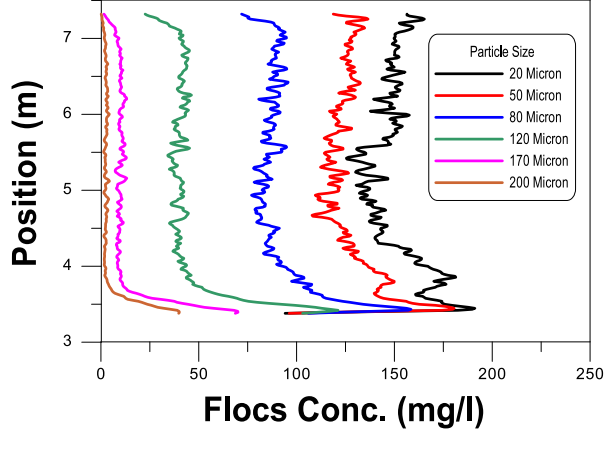
Figure 11 shows the flocs concentration at tank outlet for different particle sizes. The effluent concentration reduces as the particle size increases, the heavier particles will settle before tank outlet more than the lighter particles.

Figure 12) shows the flocs concentration profile inside the tank at radial locations for different particle class sizes. At any location inside the tank, the increase in particle size allows the flocs to settle rapidly and the flocs concentrations inside the tank will be reduced.

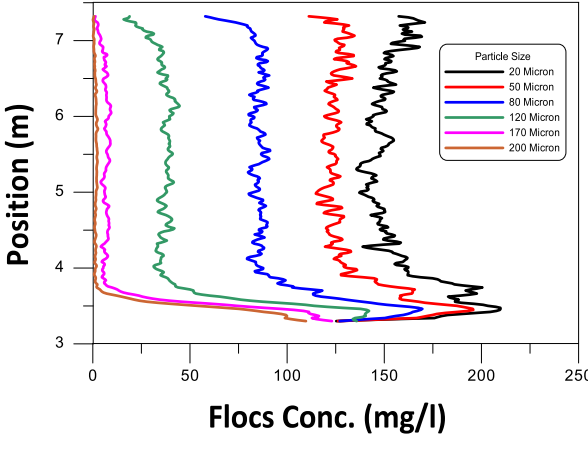
The concentration at the region close to the tank bottom will be changed according to the particle size, increase the particle size allows the solids to settle at much short distances from the inlet region. Therefore, at beginning of the settling region (at the inlet region) the concentrations at tank bottom for bigger particle size will be more than the concentration for smaller particle size and vice versa.



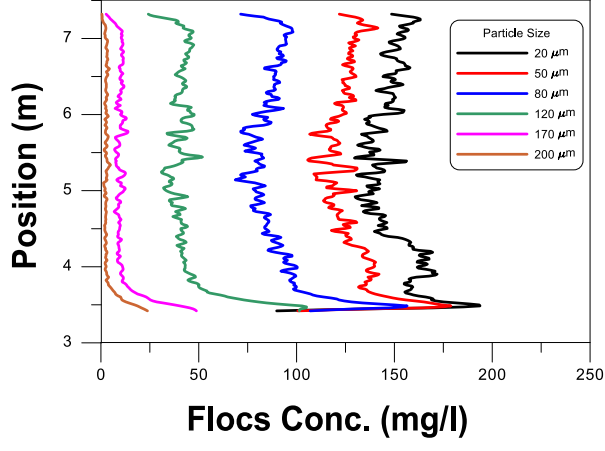
(a) at r=8.0m



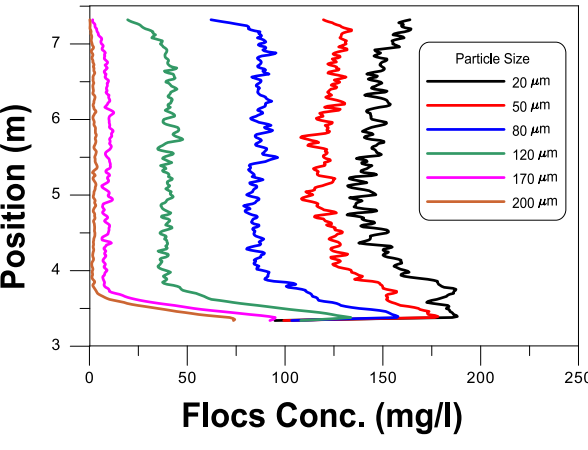
(d) at r=11



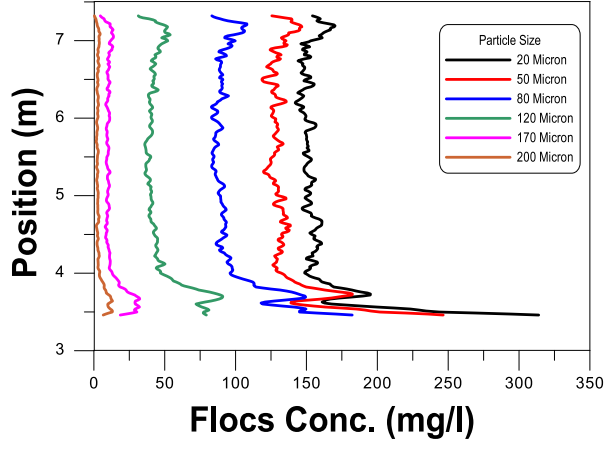
(b) at r=9.0



(e) at r=12



(c) at r=10.0



(f) at r=13

Figure 12 Flocs concentration profile inside the sedimentation tank at various radial locations for different particle sizes.

5.6 Settling Efficiency

Figure 13 presents a comparison between the simulated values of the floc size distribution in the effluent of the standard tank by Goula and et al (2008) and the present simulation work for Armant Clari-flocculator (i.e. sedimentation tank).

Figure 14 presents the predicted percents of solids settled for different tested particle size classes. As it can be inferred, the theoretical settling efficiency tends to non-zero (in fact, relatively large) values as the particles size tends to zero. This is due to the combined effect of convection (fluid velocity towards the bottom of the tank, turbulent diffusivity which is independent of the particle size and the perfect sink boundary condition). In practice it is expected that the settling efficiency decreases as particle size decreases going to a zero (or close to zero) value for Brownian particles.

The results presented in Figure 14 show an overall settling efficiency of 95.68% and 92.70%, for the sedimentation tank studied by Goula et al (2008) and the present study (Armant WTP), respectively. As it can be seen, the model predicts highly distinct concentration for different classes of particle; lower removal rate for the smallest and higher removal rate for the heaviest particles. The percentages the particle sizes more than 200 μm are very close to 100% indicating that the particles with the eight highest settling velocities would be settled almost completely regardless of the configuration used.

From Figures 13, 14 show that the results are matching with the results obtained by Goula and et al 2008.

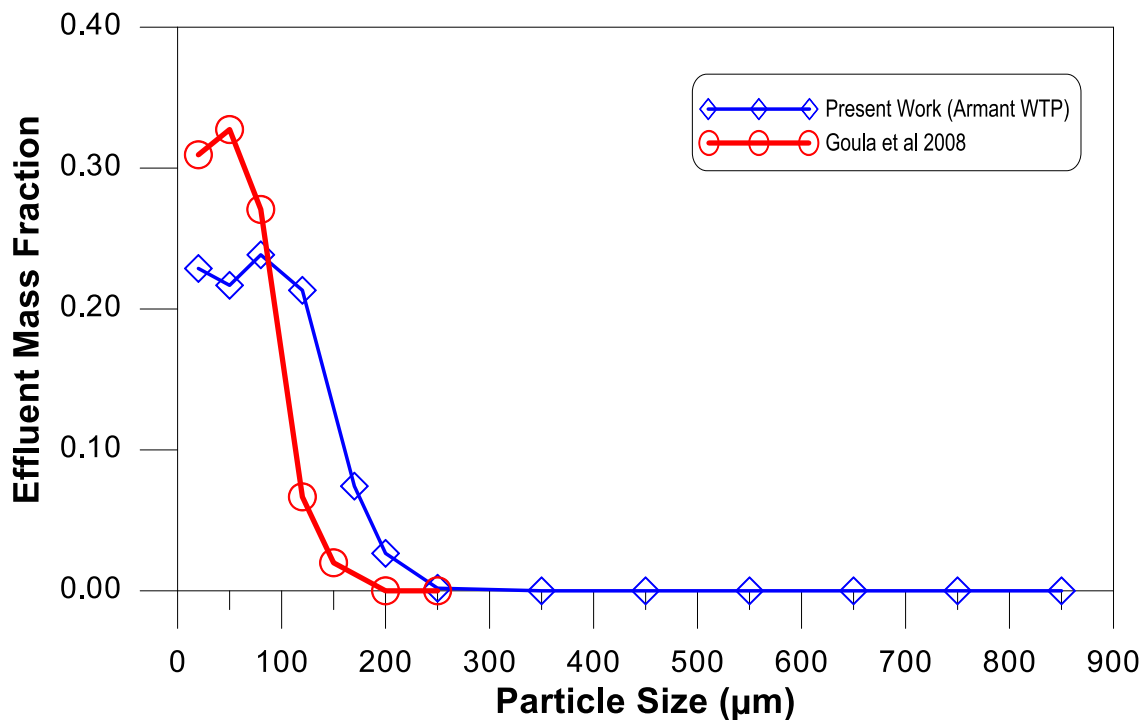


Figure 13 Simulated particle size distributions in the effluent of the sedimentation tank.

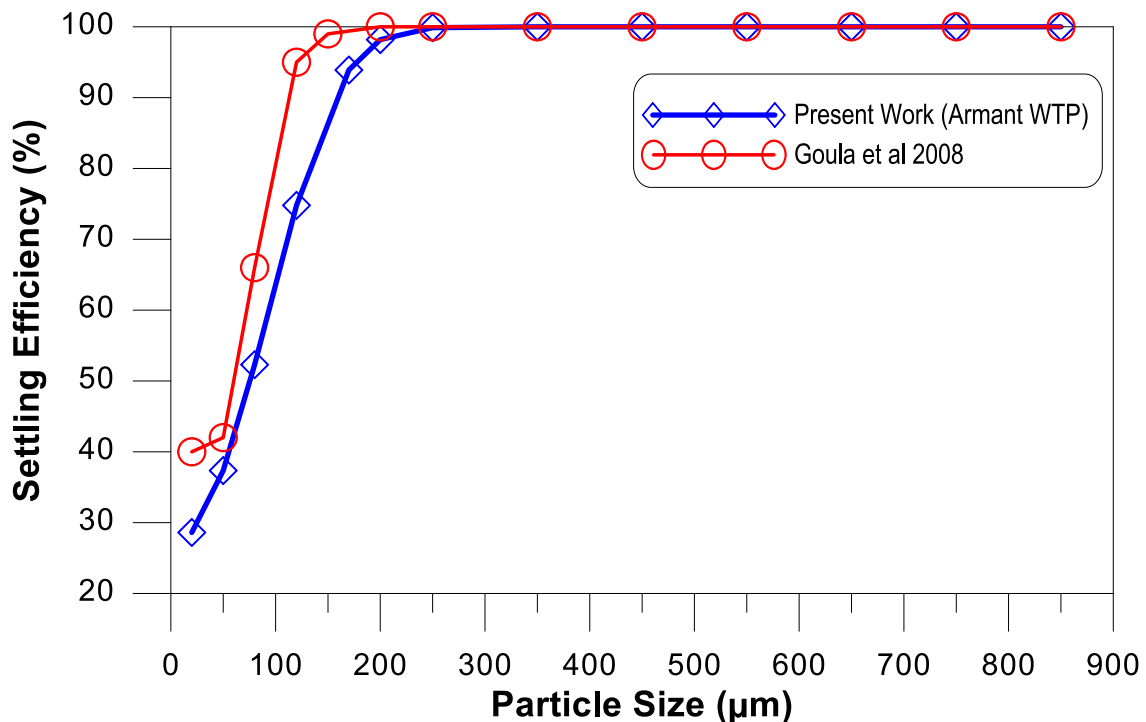


Figure 14 Predicted settling efficiency for each particle size class for the sedimentation tank.

6. CONCLUSION AND RECCOMENDATION

Numerical simulations of the existing Clariflocculator at Armant WTP were conducted to study performance as well as the removal efficiency of the sedimentation tanks and the results shows that the removal (settling) efficiency of the particle size more than 200µm are very close to 100% indicating that the particles with the highest settling velocities would be settled almost completely.

The results of the study which provide all details of the flow field and performance of the clarifier can be utilize it to enhance the design and propose the required modifications to improve the performance and settling efficiency of clarifiers

The improvement method such as plate settler, enhancement of inlet baffle and modification at flocculation zone can be proposed as future works to increase the settling efficiency for the particle sizes less than 200µm.

REFERENCES

- Abbas A. Al-Jeebory, Josef Kris and Ali H. Ghawi**, 2010, "Performance Improvement of Water Treatment Plants in Iraq by CFD Model", *Al-Qadisiya Journal for Engineering Sciences*, Vol. 3, No. 1.
- A.I. Stamou**, 1991, On the prediction of flow and mixing in settling tanks using a curvature-modified $k-\epsilon$ model, *Appl. Math. Model.* 15, pp. 351– 358.
- Athanasia M. Goula, Margaritis Kostoglou, Thodoris D. Karapantsios and Anastasios I. Zouboulis**, 2008, "The Effect of Influent Temperature Variations in a Sedimentation Tank for Potable Water Treatment— a Computational Fluid Dynamics Study", *Water Research*, Vol.42, pp. 3405 – 3414.
- Ali G. GHAW And J. Kris**, 2011, "Improvement Performance Of Secondary Clarifiers By A Computational Fluid Dynamics Model", *Slovak Journal of Civil Engineering*, Vol. XIX, No. 4, pp. 1 – 11.
- Ansys Fluent**, 2012, "Users Guide", release 14.5.
- Benedek Gy. Plo' sz , Michael Weiss, Cyril Printemps, Karim Essemiani and Jens Meinhold**, 2007, "One-Dimensional Modelling of The Secondary Clarifier factors Affecting Simulation in The Clarification Zone and The Assessment of The Thickening Flow Dependence", *Water Research*, Vol.41, pp. 3359 – 3371.
- Camp T.R**, 1946, "Sedimentation and the design of settling tanks", *Trans. ASCE*, 111(6), pp. 895-952.
- Campbell B.K. and Empie H.J.**, 2006, "Improving fluid flow in clarifiers using a highly porous media", *J. Env.Engng.*, 132(10), pp. 1249-1254.
- Cripps S.J. and Bergheim**, 2000, "Solids management and removal for intensive land-based aquaculture production systems", *J. Aqua-Cultural Engng.*, pp. 33-56.
- De Clercq, Kinnear and Vanrolleghem**, 2003, "On-line dynamic fluid velocity Profiling in secondary clarifiers", *Biomath*, Ghent University, Coupure Links 653, B-9000 Belgium.
- D.L. Huggins, R.H. Piedrahita, T. Rumsey**, 2005, Use of computational fluid dynamics (CFD) for aquaculture raceway design to increase settling effectiveness, *Aquacult. Eng.* 33 (2005) 167–180
- D. J. Burt and J. Ganeshalingam**, 2005, "Design and Optimisation of Final Clarifier Performance with CFD Modelling" Presented at the CIWEM / Aqua Enviro joint conference Design and Operation of Activated Sludge Plants.
- Long Fan, Nong Xu, Xiyong Ke and Hanchang Shi**, 2007, "Numerical Simulation of Secondary Sedimentation Tank for Urban Wastewater", *Journal of the Chinese Institute of Chemical Engineers*, Vol. 38, pp. 425–433.
- McCorquodale J. Alex, Griborio Alonso, and Georgiou Ioannis**, 2006, "Application of A CFD Model To Improve The Performance of Rectangular Clarifiers", *Proceedings of the Water Environment Federation, WEFTEC 2006: Session 1 through Session 10*, pp. 310-320(11).
- Michael Marek, Thorsten Stoesser, Philip J.W. Roberts, Volker Tbrecht and Gerhard H. Jirka**, 2007, "CFD Modelling of Turbulent Jet Mixing in a Water Storage Tank", Article, Research Gate.
- Swamee, P.K. and Tyagi**, 1996, "Design of class-I sedimentation tanks", *J. Env. Engng.*, 122(1), pp. 71-73.
- T. Matko, N. Fawcett, A. Sharp and T. Stephenson**, 1996, "Recent Progress in The Numerical Modelling of Wastewater Sedimentation Tanks", *Process Safety and Environmental Protection-ICHEME*, Vol 74, Part B, pp. 245-258.